Experimental demonstration of single-span 100-km O-band 4×50-Gb/s CWDM direct-detection transmission

Yang Hong*, Natsupa Taengnoi, Kyle R. H. Bottrill, Naresh K. Thipparapu, Yu Wang, Jayanta K. Sahu, David J. Richardson, and Periklis Petropoulos

Optoelectronics Research Centre, University of Southampton, Southampton SO17 1BJ, United Kingdom
*y.hong@soton.ac.uk

Abstract: We report on what is to the best of our knowledge the longest 50-Gb/s/λ O-band wavelength-division multiplexed (WDM) transmission. A pair of in-house built bismuth-doped fiber amplifiers (BDFAs) and the use of Kramers-Kronig detection-assisted single-sideband transmission are adopted to overcome the fiber loss and chromatic dispersion, respectively, in a reach-extended O-band coarse WDM (CWDM) system with a channel spacing of ~10 nm. Through experiments on an amplified 4×50-Gb/s/λ direct-detection system based on booster and pre-amp BDFAs, we show the superior performance of single-sideband transmission in terms of both optical signal-to-noise ratio sensitivity and uniformity in performance amongst CWDM channels relative to double-sideband transmission after both 75-km and 100-km lengths of single-mode fiber. As a result, up to 100-km reach with comparable performance at all 50-Gb/s channels was achieved without the need for in-line optical amplification.

1. Introduction

Wavelength-division multiplexed (WDM) transmission in the O-band is extensively used in short-reach optical transmission systems today, in applications ranging from data center interconnects to passive optical networks [1-2]. The use of O-band WDM direct-detection (DD) transmission has also been adopted in the standards of various bodies, including the IEEE, the International Telecommunication Union (ITU), and the multi-source agreement (MSA) [3-5]. For example, coarse WDM (CWDM) transmission using four and eight wavelengths in the O-band has been specified in IEEE 100GBASE-LR4 and 400GBASE-LR8, respectively [3]. As a result of this intense interest in high-speed O-band transmission, several research developments have emerged in recent years, relating particularly to: (i) increase in the aggregate data rate of such systems [6-14], (ii) improvement in receiver sensitivity [15-18], and (iii) extension of the transmission reach [19-22]. To boost the capacity of O-band short-haul transmission, various solutions have been investigated in the literature, including the development of high-bandwidth transceivers [6-7], and the use of advanced signal formats and associated digital signal processing (DSP), such as the probabilistically-shaped pulse amplitude modulation, discrete multitone modulation with adaptive bit loading, and spectral shaping [9-14]. With regards to improving the receiver sensitivity, the main objective is to accommodate the power budget requirement whilst increasing the data rate to 50 Gb/s/λ and beyond [15-17]. The adoption of avalanche photodetectors or receiver-side advanced DSP are considered as effective schemes to achieve this goal [15-18]. An alternative route is to introduce optical amplification to the system, and the use of commercially available semiconductor optical amplifiers (SOAs) has been reported in [17-18].

On the other hand, extension of the reach of O-band systems is necessary in order firstly, to simplify and ensure the sustainability of cloud/edge networks, and secondly, to enable the implementation of multi-band systems that will benefit from the use of an extended bandwidth

over the existing fiber infrastructure, and thus accommodate the rapidly increasing data traffic [21-26]. However, this will only be possible if suitable optical amplification technologies, capable of amplifying several high-speed WDM signals are available [19-20]. This is represented in Fig. 1, which summarizes some recent O-band WDM transmission demonstrations, and highlights the role of optical amplification in realizing transmission reaches >40 km. The figure combines results from unamplified, single-span and multi-span experiments in the O-band, as reported in the literature, and presents them with respect to the span length, i.e. the length of fiber in between optical amplifiers (where applicable). For O-band amplification, although SOAs have commonly been used, their relatively high nonlinearity and noise figure (NF) limit the transmission performance [27]. As a result, the span lengths of O-band WDM systems based on SOAs have typically been limited to shorter than 40-50 km [10, 25], and this has been true even when longer transmission distances were targeted through in-line amplification [28].
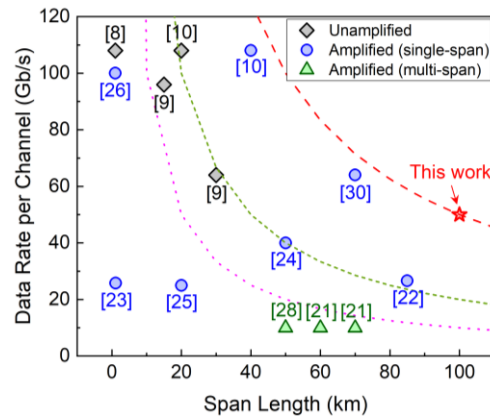

Fig. 1. Comparison of representative O-band WDM transmission demonstrations. The reference lines correspond to the rate-span length products at 1000 (purple), 2000 (green) and 5000 (red) Gb/s·km.

In addition to SOAs, other amplification solutions for the O-band mainly involve Raman amplifiers, praseodymium-doped fiber amplifiers (PDFAs), and bismuth-doped fiber amplifiers (BDFAs) [21-24, 29-31]. While the use of the Raman amplifier has been reported in Gigabit/s passive optical networks for O-band amplification [29], the implementation complexity and thereby its cost is relatively high. In addition, it also normally exhibits a high power consumption [31]. The use of PDFAs has been demonstrated for the transmission of 2×64-Gb/s signals over a 70-km length of single-mode fiber (SMF) [30]. However, PDFAs do not use a silica-glass host and are therefore also a costly solution. More importantly, PDFAs generally have a narrow gain bandwidth, and therefore are not suitable for O-band CWDM applications [31]. On the other hand, the recently emerged BDFAs are silica glass-based and can offer more than 20 dB of gain over wide bandwidths covering wavelengths in the O- and E-bands, whilst exhibiting good NF performance [20, 31]. Moreover, in contrast to SOAs, BDFAs do not impose nonlinear distortions on the amplified optical signals, hence they are better suited to the amplification of high-capacity WDM signals [27]. With the help of an in-line BDFA, up to 120-km and 140-km transmission distances were demonstrated for O-band CWDM and dense WDM transmission at 10 Gb/s/λ, respectively [21]. Using a pair of booster and pre-amplifier BDFAs, the transmission reach of an eight-channel 25-Gb/s/λ O-band CWDM system was extended to 85 km in [22].

When the reach of high-capacity O-band WDM transmission is extended, the chromatic dispersion (CD) can no longer be neglected [32-34]. This is because, even though the CD in the SMF is low at O-band wavelengths, ranging from around -5.1 to 3.8 ps/nm/km over 1260

nm to 1360 nm (average values in the specified range in the ITU G.652 standard [35]), it is cumulative along the fiber propagation length. Eventually, severe power fading will occur within the bandwidth of transmission signals when the baud rate is high enough and/or the fiber link is long enough, leading to significantly degraded transmission performance [33, 34]. This will further introduce performance uniformity issues amongst the O-band WDM channels, since the more dispersive wavelengths will suffer more, especially in the case of CWDM scenarios, where a broad spectral range is utilized.

This paper incorporates the preliminary results presented in [34], and presents a detailed literature review, further technical information, as well as additional numerical and experimental results. We have also expanded the discussion to offer a deeper insight into the prospects of BDFA-enabled amplified O-band links. We first study numerically the impact of CD on the achievable performance of O-band CWDM transmission. A 50-Gb/s/λ CWDM DD system with a channel spacing of ~10 nm using a pair of booster and pre-amplifier BDFAs is then implemented experimentally, based on which a single-sideband (SSB) WDM transmission in the O-band is demonstrated. Although the benefits of SSB transmission with Kramers-Kronig (KK) detection for combating the effects of CD have been analyzed in the C-band, SSB has so far been considered superfluous in O-band transmission. Here, we show the performance benefits of KK detection-assisted SSB quadrature phase shift keying (KK-QPSK) by comparing it with double-sideband Nyquist on-off keying (OOK) in the same system. Our results show not only that significant improvements in the optical signal-to-noise ratio (OSNR) sensitivity are achieved after transmission over 75-km and 100-km of SMF, but also that more uniform performance is obtained across the different CWDM channels. These results represent the longest O-band WDM transmission system at 50 Gb/s/λ, demonstrating a reach of up to 100 km without the use of in-line optical amplification.

2. Numerical simulation

In this section, the impact of CD on O-band CWDM transmission is numerically studied. In accord with the experimental investigations presented later in this paper, we adopted the four wavelengths of 1330.6 nm, 1343.1 nm, 1351.1 nm, and 1360.0 nm in our simulations. The CD values at the four wavelengths were assumed to be 1.5, 2.3, 3.3, and 3.8 ps/nm/km, respectively, following the specifications of standard SMFs in the ITU-G.652 standard [35]. As mentioned earlier, the main manifestation of CD in intensity-modulated (IM) optical signals is the frequency-selective power fading experienced after square-law detection. This effect imposes an upper limit on either the achievable data rate or the transmission reach of the system [33].
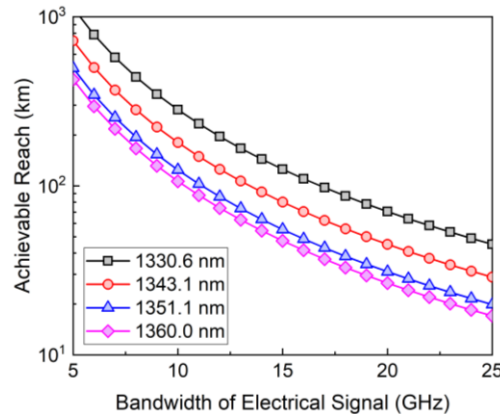

Fig. 2. Achievable reach versus bandwidth of electrical signal at the wavelengths of 1330.6 nm, 1343.1 nm, 1351.1 nm, and 1360.0 nm.

Fig. 2 shows the relation between the maximum achievable reach and the RF bandwidth of a double-sideband signal at the four considered wavelengths. Here, the achievable reach is defined as the transmission distance over which the highest frequency component of the detected electrical signal at the receiver experiences a 3-dB power fading. The maximum achievable reach can therefore be expressed as

$$L_{max} = \frac{\arccos(\sqrt{0.5}) \cdot c}{\pi \lambda^2 D f_{BW}^2} \qquad (1)$$

where the factor of 0.5 corresponds to 3-dB power fading, c is the speed of light, λ is the wavelength of the optical carrier, D is the CD value at this wavelength, and f_{BW}^2 is the bandwidth of the double-sideband signal [36].

According to Fig.2, the achievable reach differs significantly amongst the four wavelengths, and the shortest wavelength (1330.6 nm) exhibits more than 2.5 times longer reach than the most dispersive wavelength (1360.0 nm). Moreover, even for this shorter wavelength of 1330.6 nm, the achievable reach is far shorter than 100 km if we consider a signal bandwidth of 25 GHz. On the other hand, for a given reach, the signal bandwidths (i.e., the baud rates) that the four wavelengths can support also differ significantly. These limitations mean that performance uniformity of the O-band CWDM channels cannot be guaranteed when double-sideband IM transmission is adopted. In contrast, single-sideband modulation can offer benefits when longer-reach O-band CWDM transmission is targeted, since the impact of CD can be eliminated by using digital CD compensation [37].
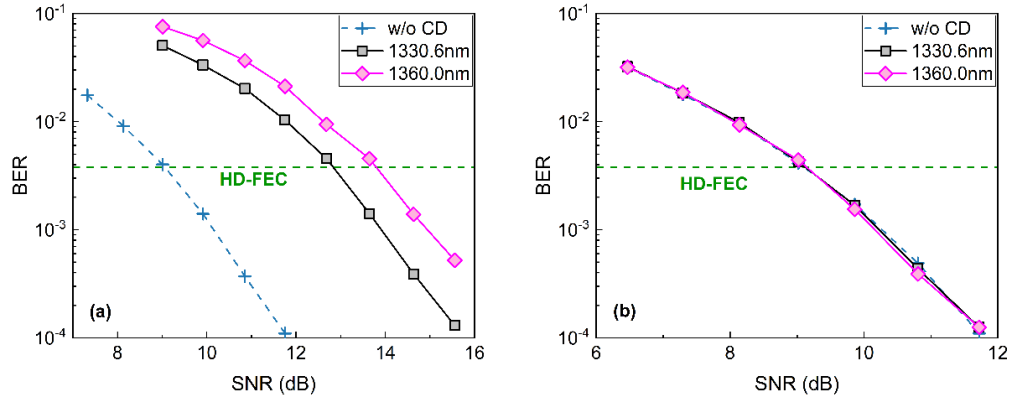

Fig. 3. Simulation results of BER versus SNR after 50-Gb/s transmission in 100-km length of SMF: (a) Nyquist OOK and (b) KK-QPSK.

To further quantify the impact of CD on O-band CDWM, we numerically studied the performance of 50-Gb/s transmission of both double-sideband Nyquist OOK and single-sideband KK-QPSK formats. The shortest and longest wavelengths mentioned above were used here (i.e., 1330.6 nm and 1360.0 nm). For simplicity, the simulated channel only encompassed the effect of CD and the additive white Gaussian noise, and the DSP of the two formats were identical to that used in the experiments (as will be detailed in Section 3). Fig. 3 shows the bit error rate (BER) versus SNR for 50-Gb/s transmission over a 100-km length of SMF using each of the two formats. We note that throughout this paper, BERs refer to pre-forward error correction (pre-FEC) BERs. For reference, we have also included the results of the zero CD case. It is seen that for the 50-Gb/s Nyquist OOK transmission shown in Fig. 3(a), the CD introduced more than 4-dB SNR penalty relative to the scenario of zero CD at the hard-decision FEC (HD-FEC) limit of 3.8×10^{-3}. In addition, it is clear that the BER performance also degraded at the longer wavelength of 1360.0 nm, due to the more severe impact of CD. In

comparison, as shown in Fig. 3(b), both channels experienced comparable BER performance in KK-QPSK transmission, with no additional penalty relative to the scenario of zero CD. This resulted from the beneficial capability of eliminating the impact of CD when the KK-QPSK format was adopted.
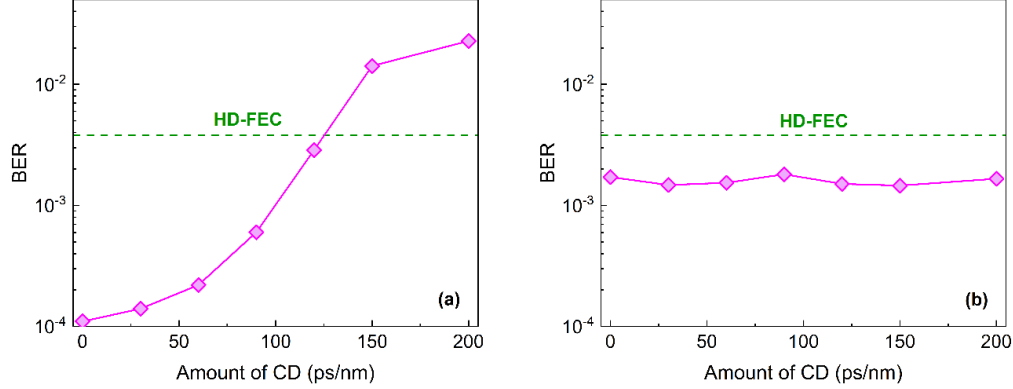

Fig. 4. Simulation results of BER versus the amount of CD for 50-Gb/s transmission at 1360.0 nm using: (a) Nyquist OOK and (b) KK-QPSK.

This advantage is further illustrated by a study of the BER evolution with CD for the two formats (Fig. 4) at the most dispersive wavelength of 1360.0 nm. The considered SNRs were around 12 dB and 10 dB for Nyquist OOK and KK-QPSK, respectively. It is seen that the BER performance of the Nyquist OOK transmission degraded quickly when increasing the amount of CD. For this value of SNR, the maximum tolerable amount of CD that resulted in a BER below the HD-FEC limit was around 120 ps/nm. In contrast, as shown in Fig. 4(b), the BER performance of the KK-QPSK transmission remained uniform regardless of the amount of CD, as expected. To experimentally quantify the relative benefits of the KK-QPSK format compared to Nyquist OOK, we also conducted four-channel WDM transmission experiments using the two formats, which will be detailed in the remainder of this paper.

3. Experimental setup

Fig. 5 shows the setup of the four-channel O-band CWDM DD system we experimented with. At the transmitter, continuous-wave lightwaves generated from four lasers operating at 1330.6 nm, 1343.1 nm, 1351.1 nm, and 1360.0 nm were used as the optical carriers for the four CWDM channels. Here, the channel spacing of our experimental CWDM system was around 10 nm, which was limited by the availability of O-band lasers and the gain bandwidth of the BDFAs. (It is worth noting that 20-nm spacing is more commonly used in O-band CWDM systems [3-5].) They were divided into odd and even channels for modulation by two independent Mach-Zehnder modulators (MZMs) to ensure channel decorrelation. After modulation, the four channels were first combined via an optical coupler, and then amplified using a booster BDFA (BDFA1). The total input power to BDFA1 was around 0 dBm. A variable optical attenuator (VOA1) was used after BDFA1 to vary the launch power into either a 75-km or 100-km long length of SMF, with the power values monitored via use of a 99:1 optical coupler. The accumulated amounts of CD at the four wavelengths used in the experiment are estimated to be around 112.5, 172.5, 247.5, 285 ps/nm, respectively, after 75-km transmission, and further increase to about 150, 230, 330, and 380 ps/nm, respectively, after 100-km transmission. After SMF transmission, another VOA (VOA2) was used to adjust the input power to the pre-amplifier BDFA (BDFA2), so as to vary the OSNR and controllably load the signal with noise at the receiver. We note that in the case of back-to-back (B2B) transmission, the combined outputs of the MZMs were directly connected to VOA2, excluding the booster BDFA1 and the SMF, as indicated by the dashed line in Fig. 5. After BDFA2, an optical bandpass filter (OBPF)

with a fixed bandwidth of 1.2 nm was used to select the channel to be tested, and a third VOA (VOA3) was used to fix the optical power at the photodetector (PD) to a constant power of around -10 dBm for all cases. The PD exhibited a 3-dB bandwidth of around 30 GHz. The OSNR at the receiver was monitored by using another 99:1 optical coupler, with 1% of the optical power being fed into an optical spectrum analyzer (OSA) whilst the remaining 99% was detected by the PD. Note that the signal power in the OSNR measurement accounted for both the optical carrier and the sideband signals. The detected electrical signal at the PD was subsequently captured by a digital storage oscilloscope (DSO, Agilent DSO-X 93204A, 30-GHz bandwidth) for further offline DSP. The overall 3-dB and 10-dB electrical bandwidths of our experimental setup were around 15 GHz and 25 GHz, respectively.
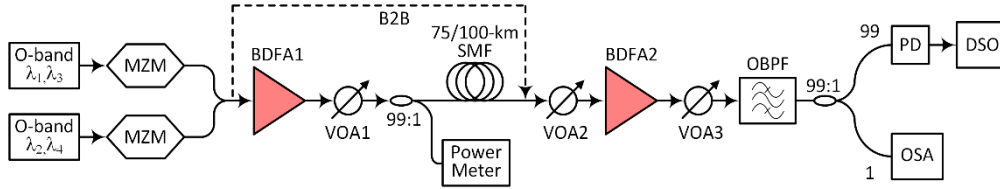

Fig. 5. Experimental setup of the 4×50-Gb/s O-band CWDM DD system using a pair of BDFAs.

We considered both a double-sideband Nyquist OOK format and a single-sideband KK-QPSK format for the O-band CWDM transmission. The gross data rates of both formats were 50 Gb/s/λ, and therefore the baud rates of the Nyquist OOK and single-sideband KK-QPSK formats were 50 GBaud and 25 GBaud, respectively. The generation of the Nyquist OOK signal included OOK mapping, up-sampling, Nyquist shaping with a square-root-raised-cosine (SRRC) filter, and down-sampling at the transmitter. The resulting signal was fed into an arbitrary waveform generator (Keysight M8196A, 30-GHz bandwidth) for analog signal generation. Correspondingly, the receiver-side DSP of the Nyquist OOK transmission included synchronization, re-sampling, matched SRRC filtering, adaptive equalization, and OOK de-mapping for BER evaluation via error counting [33]. Specifically, the T/2-spaced decision feedback equalizer (DFE) with 17 feedforward and 7 feedback taps was used in the adaptive equalization stage, in which the recursive least squares algorithm was adopted. We note that the numbers of the DFE taps were optimized to minimize the complexity without sacrificing the BER performance. Further increasing the numbers of taps would only lead to higher implementation complexity rather than a lower BER. Similar processing was conducted for the KK-QSPK signal generation, and the differences compared to the Nyquist OOK processing were: (i) a pair of orthogonal SRRC filters that were used to filter the *I* and *Q* components of the up-sampled QPSK data, followed by an up-conversion to a subcarrier frequency of 0.52 times the symbol rate, and (ii) that the down-sampled data after up-conversion were Hilbert transformed to obtain the single-sideband QPSK signal. At the receiver, 6-times up-sampling, KK detection, and CD compensation were additionally implemented in this order in the case of KK-QSPK transmission. The rest of the receiver-side DSP was nearly identical to that used in the Nyquist OOK case, apart from the orthogonal matched SRRC filtering and the down-conversion. The same equalization was applied in the KK-QPSK case to ensure a fair performance comparison with the Nyquist OOK.

We note that one dual-drive and one single-drive MZM were available when performing the experiments. Therefore, we swapped the modulators used in the odd and even channels in the SSB transmission case during our measurements, so that all WDM channels carried data signals, while the dual-drive MZM was assigned each time to the channel of interest. In this way, the dual-drive MZM (DD-MZM) was used to generate the optical SSB signals. To achieve this, the DD-MZM was biased at its quadrature point and a small optical modulation index was adopted [24]. Detailed principles of using a DD-MZM to generate optical SSB signals can be

found in [38]. A discussion on the different approaches that can be adopted for the generation of optical SSB signals will be presented later in Section 4.3. Without loss of generality, a comparison of the spectral traces of the generated optical signals after the MZM at the channel of 1330.6 nm for the Nyquist OOK and KK-QPSK cases is given in Fig. 6.
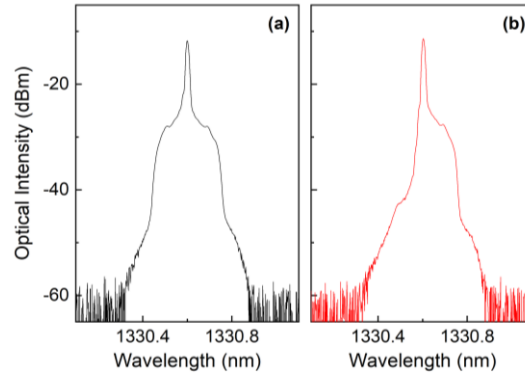

Fig. 6. Optical spectrum of the signal at the 1330.6-nm channel after the MZM in the case of: (a) Nyquist OOK transmission, and (b) KK-QPSK transmission.

Fig. 7 shows the gain performance of the two BDFAs employed in the experiments over the spectral region of 1330 nm to 1360 nm, wherein the input powers to the booster BDFA1 and pre-amplifier BDFA2 were -6 dBm and -20 dBm, respectively. It is seen that under these operating conditions, the booster BDFA1 offered a gain of around 20-dB for wavelengths between 1330 nm and 1350 nm. The gain was reduced to ~18 dB at the wavelength of 1360 nm. The pre-amplifier BDFA2 offered more than 23-dB gain under the -20-dBm input power at all the wavelengths of interest. Furthermore, a gain higher than 28 dB was achieved in the 1335-1340 nm wavelength range. More details of the in-house built BDFA, including the characterizations of its NF, saturation power, polarization-dependent gain, and pump wavelength/power, have been reported in [20, 39]. We note that BDFA technology is capable of realizing amplification over bandwidths in excess of 100 nm in this spectral region [40, 41]. Even though such an extremely broadband amplifier is not used in this work, we consider our experiments to be indicative of the potential offered by BDFAs in longer-reach O-band transmission.
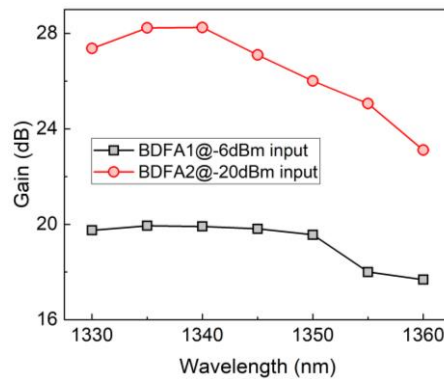

Fig. 7. Gain performance of the two BDFAs used in the experiments.

4. Experimental results

In this section, we first present the performance of the 4×50-Gb/s O-band CWDM signals in the B2B case, using either Nyquist OOK or KK-QPSK modulation. Then the results after

transmission in 75-km and 100-km lengths of SMF will be presented, including both the results of BER versus launch power at the 1330.6-nm channel and the results of BER versus OSNR at all four channels. Finally, we discuss the corresponding implementation complexity.
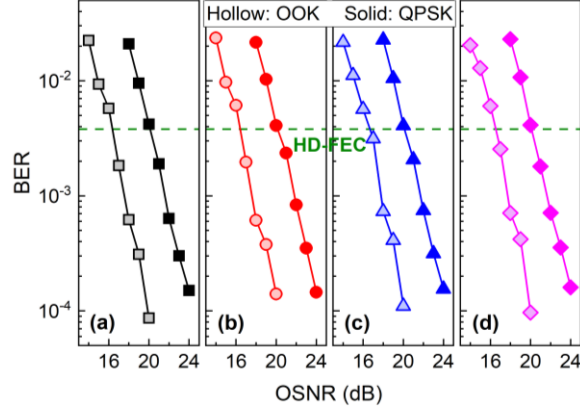
4.1 B2B transmission

Fig. 8. BER results under different OSNRs of the B2B link at (a) 1330.6 nm, (b) 1343.1 nm, (c) 1351.1 nm, and (d) 1360.0 nm.

Fig. 8 summarizes the results of BER measurements under different OSNRs at the four channels in the B2B case. All four channels exhibited a similar BER performance using either the OOK or QPSK format. Furthermore, at the HD-FEC limit, the Nyquist OOK transmission showed around ~3-dB OSNR sensitivity advantage over the KK detection-assisted QPSK transmission. This resulted from the inferior receiver sensitivity of KK detection compared to IM/DD [42, 43], as well as the non-ideal generation of the single-sideband signal using the dual-drive MZM, which provided a sideband suppression ratio of less than 20 dB, as shown in Fig. 6(b).

4.2 Transmission over 75-km and 100-km lengths of SMF

The BER performance of the 1330.6-nm channel for different total launch powers was evaluated next for the two transmission distances of 75 km and 100 km, as shown in Fig. 9. Here, all the WDM channels were active when performing the investigations of BER versus launch power, and the launch power refers to the total power of all four channels (i.e., the power of each WDM channel was 6 dB less). Without loss of generality, the corresponding performance of the first channel (i.e., 1330.6 nm) was presented. We note that under the same launch power, the OSNR conditions at the receiver were different in the 75-km and 100-km cases, due to the difference in the fiber loss. This resulted in degraded BER performance when extending the reach from 75 km to 100 km for the same launch power, as shown in Fig. 9. Furthermore, it is seen that in both cases, KK-QPSK exhibited better BER performance than Nyquist OOK. For the 75-km case, the performance gap is observed to become narrower as the power was increased. This is because the impact of the CD-induced power fading on the OOK signal was not too severe at this wavelength (Fig.2 suggests that the 3-dB bandwidth of the fiber at this distance is around 20 GHz), and thus it could be mitigated by increasing the launch power (i.e., achieving a higher OSNR at the receiver). However, a high launch power saturated the pre-amplifier BDFA2 and led to a converged BER performance for the two modulation formats. In comparison, when the reach was further extended to 100 km, it was not possible to achieve BERs below the HD-FEC limit when transmitting the OOK signals (only the soft-decision (SD-FEC) limit of 2.4×10^{-2} could be achieved), owing to the severity of the power fading at this distance, which represents the dominant factor that determined the transmission performance. By adopting the CD-tolerant single-sideband QPSK instead, a BER below the HD-FEC could be obtained at the power levels that were available.
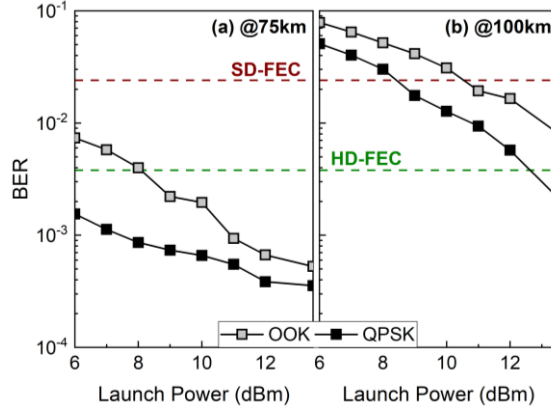
Fig. 9. BER versus total launch power at the 1330.6-nm channel: (a) after 75-km SMF, and (b) after 100-km SMF.

Furthermore, it is seen in Fig. 9 that in both cases, increasing the total launch power to a level as high as 13.5 dBm in the adopted O-band system did not lead to any BER performance degradation, which indicates that nonlinear effects in the fiber did not affect the signal performance at this power level thanks to the coarse spacing between the CWDM channels. Therefore, we kept the total launch power at 13.5 dBm and adjusted VOA2 to achieve different OSNRs at the receiver for the remaining BER evaluations.
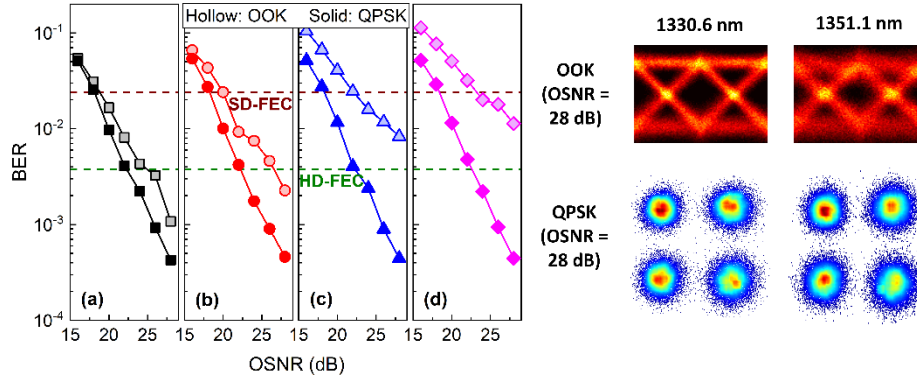

Fig. 10. BER results under different OSNRs of the CWDM system after the 75-km length of SMF: (a) 1330.6-nm, (b) 1343.1-nm, (c) 1351.1-nm, and (d) 1360.0-nm channel. Insets: recovered eye/constellation diagrams at the 1330.6-nm and 1351.1-nm channels under the OSNR of 28 dB.

Fig. 10 presents the results of BER versus OSNR for each of the four channels after transmission over 75 km of SMF and the corresponding eye/constellation diagrams under 28-dB OSNR at the 1330.6-nm and 1351.1-nm channels. In contrast to the results of the B2B link, KK-QPSK exhibited lower BERs than Nyquist OOK under the same OSNRs. Furthermore, while comparable BER performance was achieved at the four channels using KK-QPSK, the performance of the OOK signals became progressively worse as the wavelength increased (which is directly evidenced by the degraded eye opening shown in the insets of Fig. 10), resulting in the performance gaps between the two formats becoming ever wider in these cases. This was due to the more severe impact of CD-induced power fading on the OOK signals at channels with a longer wavelength, whereas the impact of CD was compensated for in the KK-QPSK transmission. As a result, KK-QPSK showed around 2-dB and 4-dB OSNR sensitivity benefits at the HD-FEC limit at the 1330.6-nm and 1343.1-nm channels, respectively. A BER below the HD-FEC limit was not achievable for the OOK signals at the two longest

wavelengths (i.e., 1351.1 nm and 1360.0 nm), even at the highest OSNR of 28 dB. In these cases, KK-QPSK offered a >6-dB sensitivity enhancement.

The electrical spectra of the detected Nyquist OOK signals at the four channels in the B2B and 75-km transmission cases are shown in Fig. 11, which confirm the increased severity of the CD-induced power fading at longer wavelengths. It is seen that in the B2B case, all four channels exhibited a similar spectral roll-off, which was induced by the high-frequency attenuation of the transceiver. In comparison, in the 75-km transmission case, all channels experienced additional power fading due to the effect of the SMF's CD. Apart from the channel at the shortest wavelength (1330.6 nm), all the other three channels exhibited a spectral null within the signal bandwidth, and the frequency of the null decreased as the wavelength (hence the value of CD) increased. We have also simulated the theoretical fading profiles after 75-km of SMF at these four wavelengths using the CD values mentioned in Section 2, which are illustrated by the curves with markers in Fig. 11. We note that the simulation of the fading profiles excluded the frequency roll-off of the system (as can be seen in the B2B spectra). Therefore, the frequencies of the spectral nulls are of interest here, as they indicate the severity of CD at different channels. As shown in Fig. 11, the locations of the spectral nulls are in agreement with the experimentally obtained values.
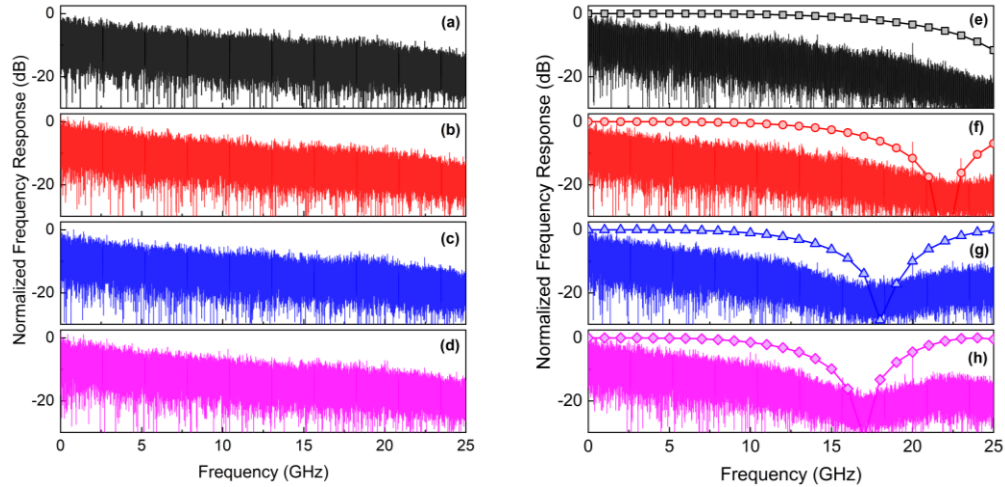

Fig. 11. Experimentally obtained electrical spectra of the Nyquist OOK signals in the B2B case: (a)-(d) 1330.6 nm to 1360.0 nm; and in the 75-km SMF case: (e)-(h) 1330.6 nm to 1360.0 nm. Curves with markers in (e)-(h): the corresponding numerically simulated profiles of CD-induced power fading.
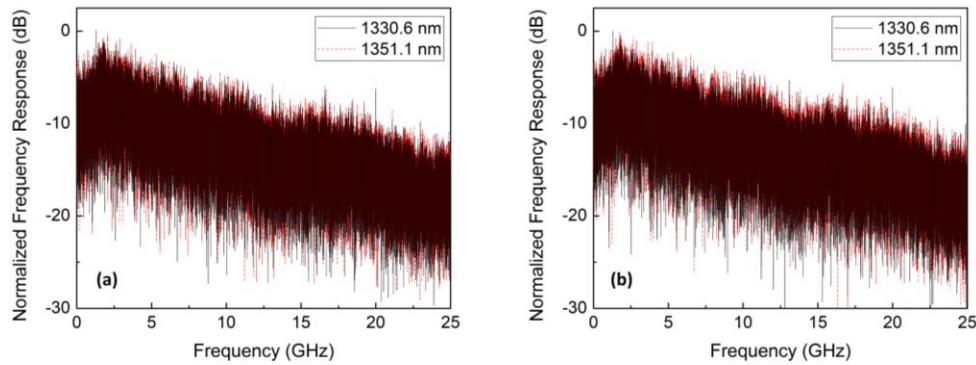

Fig. 12. Electrical spectra of the detected QPSK signals at 1330.6-nm and 1351.1-nm channels in the (a) B2B case; and (b) 75-km SMF case.

Unlike the case of double-sideband Nyquist OOK transmission, the KK-QSPK transmission did not suffer from the issue of CD-induced power fading. As a result, in contrast to the results in the Nyquist OOK transmission, all four WDM channels exhibited comparable spectra in both B2B and after fiber transmission cases. Without loss of generality, we have compared the electrical spectra of the odd channels (i.e., 1330.6 nm and 1351.1 nm) in the B2B and 75-km SMF transmission cases in Fig. 12 to illustrate this benefit obtained by the use of the KK-QPSK format. The spectra of the two channels in both cases are comparable to each other. Furthermore, it can also be concluded that the roll-off of the spectra in the 75-km transmission case is indicative of the bandwidth limitation of the transceiver rather than the impact of CD, by comparing them with that in the B2B case shown in Fig. 12(a).

Finally, we extended the reach of the O-band CWDM transmission to 100 km and investigated the BER performance of the four channels under different OSNRs. The corresponding results are presented in Fig. 13. It is seen that similar to the 75-km case, when Nyquist OOK was used, the BER performance of the channels at a longer wavelength was worse than those at a shorter wavelength. Again, this is clearly indicated by the inferior quality of the eye diagram at the 1351.1-nm channel compared to that at 1330.6 nm, as shown in the insets in Fig. 13. Furthermore, none of the four channels exhibited a BERs below the HD-FEC limit, and the lowest BERs of the two longer-wavelength channels (i.e., 1351.1 nm and 1360.0 nm) were even above the SD-FEC limit at the highest OSNR value that was available in our experiment.
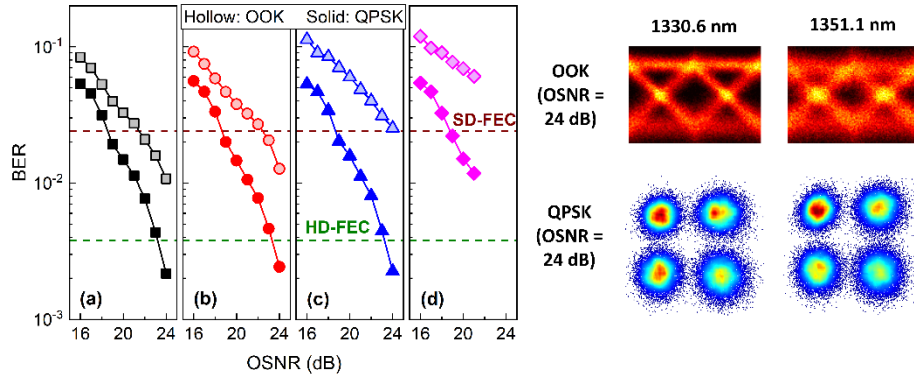

Fig. 13. BER results under different OSNRs of the CWDM system after 100-km length of SMF: (a) 1330.6-nm, (b) 1343.1-nm, (c) 1351.1-nm, and (d) 1360.0-nm channel. Insets: recovered eye/constellation diagrams at the 1330.6-nm and 1351.1-nm channels under the OSNR of 24 dB.

By using KK-QPSK instead, a similar BER performance was achieved at the four WDM channels, which also resulted in a significant improvement relative to the OOK transmission. It is noted that this performance of the KK-QPSK signals at 100 km is also comparable to the corresponding results at 75 km (see Fig. 10), which once again is thanks to the capability of CD compensation when adopting this format. Finally, it is noted that the lower gain of the two BDFAs at the wavelength of 1360.0 nm (refer to Fig. 7) restricted us from obtaining an OSNR beyond 21 dB. Nevertheless, the BER curve shows similar performance to the remaining channels at lower OSNRs and the lowest achieved BER was well below the SD-FEC limit.

4.3 Discussions

While it is clearly demonstrated that single-sideband KK-QPSK simultaneously provides significantly better BER performance and enhanced uniformity amongst the different CWDM channels, its implementation complexity/cost is also higher than that of the double-sideband Nyquist OOK. Here, we discuss feasible solutions to reduce the complexity/cost of the single-sideband KK scheme towards its practical use in O-band CWDM systems.

The key difference between the two types of formats in terms of hardware is that the generation of the single-sideband signal will ideally require the use of an IQ modulator, which is more costly than a single-drive MZM as used in the case of double-sideband signal generation. However, it is possible to use a DD-MZM instead to generate single-sideband signals (as we have demonstrated in this work), and this solution can reduce the costs by as much as 1/3 compared to the IQ modulator-based method [38]. Furthermore, it has been recently demonstrated that optical single-sideband signals can also be realized by dual-modulation of a directly modulated laser and an electro-absorption modulator. This offers the possibility of implementing the optical single-sideband transmitter with a monolithically integrated semiconductor device, through which the implementation cost can be further significantly reduced [44]. Regarding the complexity of offline DSP, various efforts have been made in the literature to relax the computational requirements of KK detection. For example, both an upsampling-free approach [43] and a low-complexity digital implementation of KK detection [45] have been reported, offering promising routes towards computationally efficient realizations.

It is also worth noting that current research efforts push DD transmission to higher data rates, targeting 100G/λ or 200G/λ [8, 11, 17]. As has been clearly indicated in this work, CD becomes a limiting factor for longer-reach O-band IM/DD transmission, and this will be even more pronounced at these higher signal rates. Therefore, we anticipate that DD schemes that can effectively combat/eliminate the CD effect, such as the KK detection-assisted SSB transmission considered in this work, will be desirable in future O-band WDM systems targeting higher baud rates and longer transmission distances.

5. Conclusions

In this work, we demonstrated up to 100-km 4×50-Gb/s O-band CWDM (~10-nm spacing) DD transmission without the use of in-line optical amplification, which represents the longest O-band WDM transmission at 50-Gb/s/λ to date. Specifically, we showed that while the loss of the SMF could be compensated for by using a booster and pre-amplifier BDFA pair, the CD of the SMF emerges as the limiting factor for both BER performance and performance uniformity in longer-reach O-band CWDM DD systems. To overcome this limitation, we demonstrated a single-sideband WDM transmission in the O-band and compared its performance with that of double-sideband transmission. The experimental results showed that significantly better OSNR sensitivity at the receiver could be achieved by using single-sideband KK-QPSK instead of the double-sideband Nyquist OOK format at both 75-km and 100-km transmission distances. Moreover, the use of single-sideband KK-QPSK also offered superior uniformity in the performance of the different CWDM channels, especially when compared to the double-sideband Nyquist OOK transmission. We believe that our results provide useful insights and show a viable route towards future longer-reach high-speed O-band CWDM systems.

Disclosures. The authors declare no conflicts of interest.

Data availability. Data underlying the results presented in this paper are available in Ref. [46].

References

1. D.V. Plant, M. Morsy-Osman, and M. Chagnon, "Optical communication systems for datacenter networks," in *Proc. of OFC*, (*Optica*, 2017), paper W3B.1.
2. F.J. Effenberger, "PON standardisation status and future prospects," in *Proc. of ECOC*, (*IEEE*, 2019), paper M.2.F.1.
3. IEEE 802.3 Ethernet working group, (*IEEE*, 2021). https://www.ieee802.org/3/.
4. M. Sysak, J. Johnson, D. Lewis, and C. Cole, "CW-WDM MSA technical specifications," (*MSA*, 2021). https://cw-wdm.org/.
5. ITU-G.694.2: Spectral grids for WDM applications: CWDM wavelength grid, (*ITU*, 2003).

6. M. Jacques, Z. Xing, A. Samani, X. Li, E. El-Fiky, S. Alam, O. Carpentier, P.C. Koh, and D.V. Plant, "Net 212.5 Gbit/s transmission in O-band with a SiP MZM, one driver and linear equalization," in *Proc. of OFC*, (*Optica*, 2020), paper Th4A.3.

7. N.P. Diamantopoulos, H. Yamazaki, S. Yamaoka, M. Nagatani, H. Nishi, H. Tanobe, R. Nakao, T. Fujii, K. Takeda, T. Kakitsuka, H. Wakita, M. Ida, H. Nosaka, F. Koyama, Y. Miyamoto, and S. Matsuo, "Net 321.24-Gb/s IMDD transmission based on a >100-GHz bandwidth directly-modulated laser," in *Proc. of OFC*, (*Optica*, 2020), paper Th4C.1.

8. L. Chorchos, and J.P. Turkiewicz, "O-Band 8×100G data transmission with 240 GHz channel spacing," *IEEE Commun. Lett.*, **23**(12), 2288-2291 (2019).

9. D. Li, L. Deng, Y. Ye, Y. Zhang, H. Song, M. Cheng, S. Fu, M. Tang, and D. Liu, "Amplifier-free 4×96 Gb/s PAM8 transmission enabled by modified Volterra equalizer for short-reach applications using directly modulated lasers," *Opt. Express*, **27**(13), 17927-17939 (2019).

10. T. Zuo, A. Tatarczak, M.I. Olmedo, J. Estaran, J.B. Jensen, Q. Zhong, X. Xu, and I.T. Monroy, "O-band 400 Gbit/s client side optical transmission link," in *Proc. of OFC*, (*Optica*, 2014), paper M2E.4.

11. K. Wang, J. Zhang, M. Zhao, W. Zhou, L. Zhao, and J. Yu, "High-speed PS-PAM8 transmission in a four-lane IM/DD system using SOA at O-Band for 800G DCI," *IEEE Photon. Technol. Lett.*, **32**(6), 293-296 (2020).

12. D. Zou, F. Li, W. Wang, Z. Li, and Z. Li, "Amplifier-less transmission of beyond 100-Gbit/s/λ signal for 40-km DCI-Edge with 10G-class O-band DML," *J. Lightw. Technol.*, **38**(20), 5649-5655 (2020).

13. S. Yamamoto, H. Taniguchi, M. Nakamura, and Y. Kisaka, "O-Band 10-km transmission of 93-Gbaud PAM4 signal using spectral shaping technique based on nonlinear differential coding with 1-tap precoding," in *Proc. of OFC*, (*Optica*, 2020), paper T3I.3.

14. A. Masuda, S. Yamamoto, H. Taniguchi, and M. Fukutoku, "Achievement of 90-Gbaud PAM-4 with MLSE based on 2nd order Volterra filter and 2.88-Tb/s O-band transmission using 4-λ LAN-WDM and 4-Core fiber SDM," in *Proc. of OFC*, (*Optica*, 2018), paper Th1F.3.

15. K. Zhong, X. Zhou, Y. Wang, J. Huo, H. Zhang, L. Zeng, C. Yu, A.P.T. Lau, and C. Lu, "Amplifier-less transmission of 56Gbit/s PAM4 over 60km using 25Gbps EML and APD," in *Proc. of OFC*, (*Optica*, 2017), paper Tu2D.1.

16. M. Tao, L. Zhou, H. Zeng, S. Li, and X. Liu, "50-Gb/s/λ TDM-PON based on 10G DML and 10G APD supporting PR10 link loss budget after 20-km downstream transmission in the O-band," in *Proc. of OFC*, (*Optica*, 2017), paper Tu3G.2.

17. J. Zhang, J. Yu, H. Chien, J.S. Wey, M. Kong, X. Xin, and Y. Zhang, "Demonstration of 100-Gb/s/λ PAM-4 TDM-PON Supporting 29-dB Power Budget with 50-km Reach Using 10G-class O-band DML Transmitters," in *Proc. of OFC*, (*Optica*, 2019), paper Th4C.3.

18. K. Wang, J. Zhang, Y. Wei, L. Zhao, W. Zhou, M. Zhao, J. Xiao, X. Pan, B. Liu, X. Xin, L. Zhang, Y. Zhang, and J. Yu, "100-Gbit/s/λ PAM-4 signal transmission over 80-km SSMF based on an 18-GHz EML at O-band," in *Proc. of OFC*, (*Optica*, 2020), paper Th1D.5.

19. E.M. Dianov, "Amplification in extended transmission bands using bismuth-doped optical fibers," *J. Lightw. Technol.*, **31**(4), 681-688 (2013).

20. N.K. Thipparapu, A.A. Umnikov, P. Barua, and J.K. Sahu, "Bi-doped fiber amplifier with a flat gain of 25 dB operating in the wavelength band 1320–1360 nm," *Opt. Lett.*, **41**(7), 1518-1521 (2016).

21. N. Taengnoi, K.R.H. Bottrill, N.K. Thipparapu, A.A. Umnikov, J.K. Sahu, P. Petropoulos, and D.J. Richardson, "WDM transmission with in-line amplification at 1.3 µm using a Bi-doped fiber amplifier," *J. Lightw. Technol.*, **37**(8), 1826-1830 (2019).

22. V. Mikhailov, M.A. Melkumov, D. Inniss, A.M. Khegai, K.E. Riumkin, S.V. Firstov, F.V. Afanasiev, M.F. Yan, Y. Sun, J. Luo, G.S. Puc, S.D. Shenk, R.S. Windeler, P.S. Westbrook, R.L. Lingle, E.M. Dianov, and D.J. DiGiovanni, "Simple broadband bismuth doped fiber amplifier (BDFA) to extend O-band transmission reach and capacity," in *Proc. of OFC*, (*Optica*, 2019), paper M1J.4.

23. T. Hayashi, T. Nakanishi, K. Hirashima, O. Shimakawa, F. Sato, K. Koyama, A. Furuya, Y. Murakami, and T. Sasaki, "125-µm-cladding eight-core multi-core fiber realizing ultra-high-density cable suitable for O-band short-reach optical interconnects," *J. Lightw. Technol.*, **34**(1), 85-92 (2016).

24. Y. Hong, K.R.H. Bottrill, N. Taengnoi, N.K. Thipparapu, Y. Wang, A.A. Umnikov, J.K. Sahu, D.J. Richardson, and P. Petropoulos, "Experimental demonstration of dual O+C-band WDM transmission over 50-km SSMF with direct detection," *J. Lightw. Technol.*, **38**(8), 2278-2284 (2020).

25. L. Xue, L. Yi, H. Ji, P. Li, and W. Hu, "Symmetric 100-Gb/s TWDM-PON in O-Band based on 10G-class optical devices enabled by dispersion-supported equalization," *J. Lightw. Technol.*, **36**(2), 580-586 (2018).

26. Y. Hong, H. Sakr, N. Taengnoi, K.R.H. Bottrill, T.D. Bradley, J.R. Hayes, G.T. Jasion, H. Kim, N.K. Thipparapu, Y. Wang, A.A. Umnikov, J.K. Sahu, F. Poletti, P. Petropoulos, and D.J. Richardson, "Multi-band direct-detection transmission over an ultrawide bandwidth hollow-core NANF," *J. Lightw. Technol.*, **38**(10), 2849-2857 (2020).

27. N. Taengnoi, K.R.H. Bottrill, Y. Hong, N.K. Thipparapu, C. Lacava, J.K. Sahu, D.J. Richardson, and P. Petropoulos, "4-Level alternate-mark-inversion for reach extension in the O-band spectral region," *J. Lightw. Technol.*, **39**(9), 2847-2853 (2021).

28. J.P. Turkiewicz, M.T. Hill, G.D. Khoe, and H. Waardt, "Cost-effective transmission concept for LAN/MAN/SAN applications," in *Proc. of ECOC*, (*IEEE*, 2005), paper Th1.4.2.

29. B. Zhu, and D. Nesset, "GPON reach extension to 60 km with entirely passive fibre plant using Raman amplification," in *Proc. of ECOC*, (*IEEE*, 2009), paper 8.5.5.

30. F. Gao, S. Zhou, X. Li, S. Fu, L. Deng, M. Tang, D. Liu, and Q. Yang, "2 × 64 Gb/s PAM-4 transmission over 70 km SSMF using O-band 18G-class directly modulated lasers (DMLs)," *Opt. Express*, **25**(7), 7230-7237 (2017).
31. V. Mikhailov, J. Luo, D. Inniss, M. Yan, Y. Sun, G.S. Puc, R.S. Windeler, P.S. Westbrook, Y. Dulashko, and D.J. DiGiovanni, "Amplified transmission beyond C- and L- bands: doped fibre amplifiers for 1250-1450 nm range," in *Proc. of ECOC*, (*IEEE*, 2020), paper Mo1E-1.
32. J.P. Turkiewicz, "Analysis of the SSMF zero-dispersion wavelength location and its influence on high capacity 1310 nm transmission," in *Proc. of OFC*, (*Optica*, 2013), paper JW2A.06.
33. Y. Hong, K.R.H. Bottrill, N. Taengnoi, N.K. Thipparapu, Y. Wang, J.K. Sahu, D.J. Richardson, and P. Petropoulos, "Numerical and experimental study on the impact of chromatic dispersion on O-band direct-detection transmission," *Appl. Opt*., **60**(15), 4383-4390 (2021).
34. Y. Hong, N. Taengnoi, K.R.H. Bottrill, N.K. Thipparapu, Y. Wang, J.K. Sahu, D.J. Richardson, and P. Petropoulos, "Experimental demonstration of 50-Gb/s/λ O-band CWDM direct-detection transmission over 100-km SMF," in *Proc. of ACP*, (*Optica*, 2021), paper W1B.2.
35. ITU-G.652: Characteristics of a single-mode optical fibre and cable, (*ITU*, 2016).
36. X. Chen, C. Antonelli, A. Mecozzi, D. Che, and W. Shieh, "High-capacity direct-detection systems," in *Optical Fiber Telecommunications VII* (Academic, 2020), Chapter 10.
37. A. Mecozzi, C. Antonelli, and M. Shtaif, "Kramers–Kronig coherent receiver," *Optica*, **3**(11), 1220-1227 (2016).
38. L. Zhang, T. Zuo, Y. Mao, Q. Zhang, E. Zhou, G.N. Liu, and X. Xu, "Beyond 100-Gb/s transmission over 80-km SMF using direct-detection SSB-DMT at C-Band," *J. Lightw. Technol*., **34**(2), 723-729 (2016).
39. N. Taengnoi, K.R.H. Bottrill, Y. Hong, Y. Wang, N.K. Thipparapu, J.K. Sahu, P. Petropoulos, and D.J. Richardson, "Experimental characterization of an O-band bismuth-doped fiber amplifier," *Opt. Express*, **29**(10), 15345-15355 (2021).
40. Y. Wang, N.K. Thipparapu, D.J. Richardson, and J.K. Sahu, "Ultra-broadband bismuth-doped fiber amplifier covering a 115-nm bandwidth in the O and E bands," *J. Lightw. Technol*., **39**(3), 795-800 (2021).
41. Y. Ososkov, A. Khegai, S. Firstov, K. Riumkin, S. Alyshev, A. Kharakhordin, A. Lobanov, A. Guryanov, and M. Melkumov, "Pump-efficient flattop O+E-bands bismuth-doped fiber amplifier with 116 nm -3 dB gain bandwidth," *Opt. Express*, **29**(26), 44138-44145 (2021).
42. B. Sun, D. Che, H. Ji, and W. Shieh, "Towards low carrier-to-signal power ratio for Kramers-Kronig receiver" in *Proc. of OFC*, (*Optica*, 2019), paper M1H.6.
43. T. Bo, and H. Kim, "Kramers-Kronig receiver operable without digital upsampling," *Opt. Express*, **26**(11), 13810-13818 (2018).
44. T. Bo, and H. Kim, "Monolithically integrable optical single sideband transmitter for low-cost, high-density optical interconnects," in *Proc. SPIE* 11692, *Optical Interconnects XXI*, (*SPIE*, 2021), paper 1169206.
45. C. Füllner, M.M.H. Adib, S. Wolf, J.N. Kemal, W. Freude, C. Koos, and S. Randel, "Complexity analysis of the Kramers–Kronig receiver," *J. Lightw. Technol*., **37**(17), 4295-4307 (2019).
46. Y. Hong, N. Taengnoi, K.R.H. Bottrill, N.K. Thipparapu, Y. Wang, J.K. Sahu, D.J. Richardson, and P. Petropoulos, "Dataset for: Experimental demonstration of single-span 100-km O-band 4×50-Gb/s CWDM direct-detection transmission," (University of Southampton, 2022). https://doi.org/10.5258/SOTON/D2299.